

Article

New Polymorph of β -Cyclodextrin with a Higher Bioavailability

Askar K. Gatiatulin *, Ilya S. Balakhontsev , Sofia M. Talashmanova, Marat A. Ziganshin 
and Valery V. Gorbachuk 

A.M. Butlerov Institute of Chemistry, Kazan Federal University, 18 Kremlevskaya, 420008 Kazan, Russia; marat.ziganshin@kpfu.ru (M.A.Z.); valery.gorbachuk@kpfu.ru (V.V.G.)

* Correspondence: agatiatu@kpfu.ru

Abstract: A new polymorph of anhydrous β -cyclodextrin (polymorph III) was obtained and characterized for the first time using powder X-ray diffraction, infrared spectroscopy, and thermal analysis. The solution enthalpy and time of dissolution in water were determined using solution calorimetry for this polymorph and compared with those of the dried commercial form of β -cyclodextrin (polymorph I), its amorphous form, and 2-hydroxypropyl- β -cyclodextrin. The specific heat capacities of polymorphs I and III were determined using differential scanning calorimetry across a wide range of temperatures, providing enthalpy and Gibbs energy values for the polymorphic transition at 298 K. The affinities of polymorph III and 2-hydroxypropyl- β -cyclodextrin for water were characterized by determining their hydration isotherms, which provided values of hydration Gibbs energy. Being energy-rich, the new-found polymorph of β -cyclodextrin has a significantly higher dissolution rate and an increased affinity for water compared with the dried commercial form of β -cyclodextrin. These properties render the new polymorph promising in industrial applications for guest inclusion in aqueous solutions and pastes, and may be a desirable alternative for water-soluble β -cyclodextrin derivatives.

Keywords: beta-cyclodextrin; polymorphism; bioavailability; polymorphic transition; dissolution rate



Citation: Gatiatulin, A.K.; Balakhontsev, I.S.; Talashmanova, S.M.; Ziganshin, M.A.; Gorbachuk, V.V. New Polymorph of β -Cyclodextrin with a Higher Bioavailability. *Chemistry* **2024**, *6*, 51–61. <https://doi.org/10.3390/chemistry6010003>

Academic Editor: Craig Rice

Received: 20 November 2023

Revised: 15 December 2023

Accepted: 20 December 2023

Published: 23 December 2023



Copyright: © 2023 by the authors. Licensee MDPI, Basel, Switzerland. This article is an open access article distributed under the terms and conditions of the Creative Commons Attribution (CC BY) license (<https://creativecommons.org/licenses/by/4.0/>).

1. Introduction

The solubility of natural cyclodextrins is a key issue when they are used to reduce the negative effects of substances dissolved in water. Natural cyclodextrins are widely applied in pharmaceuticals, the food industry, textiles, and cosmetics [1–4] because of their ability to encapsulate various guests into their molecular cavity. The most widely used cyclodextrin is β -cyclodextrin (β CD), which accounts for approximately half of pharmaceutical applications [5]. An important property of cyclodextrins is their ability to solubilize poorly soluble drugs [6,7], which requires a cyclodextrin form with a high dissolution rate. This is a problem for β CD, which has a relatively poor solubility and slow rate of dissolution in water [8]. Increased dissolution kinetics can be achieved using the metastable polymorphic form of the substance [9,10]. Thus, a search for high-energy polymorphic forms of β CD may be of practical importance [11].

Polymorphism of guest-free β CD is significantly less studied than crystalline patterns of its inclusion compounds, which show a wide variety of packing types [12–14]. A relatively stable form of a β CD hydrate with low energy and solubility was prepared from an aqueous solution heated with a laser beam [15]. A channel-type (columnar) polymorph (named in this work as polymorph II) of anhydrous β CD was formed via precipitation from an acetone-water solution [16] and via the treatment of polymer inclusion complexes with organic solvents [17]. This polymorph has a different packing type [17] than the polymorph I prepared by drying a commercial β CD hydrate [18,19]. In Table 1, the literature information available for both polymorphs I and II is presented. Some data on β CD without guest and water can be found in the CCDC database, e.g., No. 762697, WEWTOJ, but they present a host packing in an inclusion compound where disordered

molecules of the guest and solvent were removed with software methods [20]. Generally, anhydrous β CD cannot be studied using single-crystal X-ray diffraction (SCXRD) because its crystals tend to crack during drying [21,22].

Table 1. Literature data regarding the polymorphs of anhydrous β CD.

Polymorph	I (Cage-Type)	II (Channel-Type)
Preparation method	Drying of β CD hydrate (form I)	Precipitation from an acetone-water solution [16]; treatment of polymer inclusion complexes with organic solvents [17]
Characteristic PXRD peaks (2θ), °	5.5, 6.5, 9.6, 11.0, 12.9, 13.5, 14.1, 16.9, 18.2, 22.3 [18,19]	7.2, 11.9, 18.1 [17]
Crystal system	Monoclinic [23]	Hexagonal [17]
Onset point of thermal degradation, K	540 ^a [24]	478–483 ^b [17]

^a at a heating rate of 10 K min⁻¹; ^b at a heating rate of 20 K min⁻¹.

The phase transition in anhydrous β CD was previously observed in a DSC experiment at 483–513 K [25] but the nature of this transition was not investigated. In the present work, the product obtained by heating dry β CD to 508 K was first characterized as a new polymorph based on its thermal stability, heat capacity, thermokinetics of the corresponding polymorphic transition, powder XRD pattern, hydration isotherm, and rate and enthalpy of dissolution in water. In addition, the dissolution properties of 2-hydroxypropyl- β -cyclodextrin (HP β CD), which are widely used for solubilization and guest inclusion in solutions [6,26,27], and amorphous β CD were studied to reveal the advantages of the new β CD polymorph.

2. Materials and Methods

2.1. Materials

β -cyclodextrin (β CD), Wacker Chemie AG, Burghausen, Germany, Merck Cat. No. W402826, and (2-hydroxypropyl)- β -cyclodextrin (HP β CD, MW ~1540, with a substitution degree of 1.0), Merck, Darmstadt, Germany, Cat. No. 389145 were dried before the experiments for 8 h in a vacuum of 100 Pa at 393 K. For β CD, this produced the initial anhydrous form (polymorph I). In dried CDs, the hydration level was less than 1% wt. according to thermogravimetry data. To prepare the high-temperature polymorph (polymorph III), the initial form (polymorph I) was heated to 508 K in a thermal analyzer (see below) in an argon flow of 75 mL min⁻¹ at a rate of 10 K min⁻¹ and then cooled immediately to 303 K at the same rate. For the PXRD measurement with the indexing of the obtained pattern, a larger amount of polymorph III was prepared by heating polymorph I at 505 K for 5 min in a ventilated oven and then cooling it in air to room temperature in the presence of a desiccant (3 Å molecular sieves).

The amorphous β CD was prepared by ball milling the initially dried β CD using a vibration ball mill Narva DDR GM 9458 (30 W, 50 Hz) and drying for 8 h in a vacuum of 100 Pa at 393 K.

To determine the hydration isotherms via CDs and the X-ray powder diffractograms of the β CD hydrates, the samples of anhydrous CDs were equilibrated for 120 h at 298 K, with the vapors of the saturated aqueous solutions of different inorganic compounds having a known water activity (humidity) or with saturated water vapor, as described previously [23]. The change in mass due to the hydration of the CD samples was determined gravimetrically. To recrystallize in the water vapor, the anhydrous β CD sample was equilibrated with the saturated vapor of distilled water for 24 h. To recrystallize from the aqueous solution, 30 mg of the dry β CD polymorph was dissolved in 2 mL of distilled water at room temperature.

The solutions in both cases were kept in the air at room temperature until the powders of the β CD hydrate were formed.

2.2. Thermal Analysis and Thermal Kinetics

For the thermal analysis, a combined method of thermogravimetry and differential scanning calorimetry (TG/DSC) was applied using a thermal analyzer STA 449 C Jupiter (Netzsch, Selb, Germany). The samples were heated at a rate of 10 K min^{-1} in an argon flow of 75 mL min^{-1} . In the full cycle TG/DSC experiment, the sample was also cooled at 10 K min^{-1} in the same argon flow. To obtain the kinetic parameters, heating rates of 4, 10, and 30 K min^{-1} were used under the same conditions. From the data obtained in this experiment, the kinetic parameters of the polymorphic transition were calculated using Netzsch Thermokinetics 3.1 software.

The heat capacities of the β CD polymorphs were measured using a DSC204 F1 Phoenix (Netzsch, Selb, Germany) calorimeter with a sapphire disk as a standard as described elsewhere [28].

2.3. Powder X-ray Diffraction (PXRD)

Powder diffractograms were obtained using a MiniFlex 600 (Rigaku, Tokyo, Japan) diffractometer with a D/teX Ultra detector. In this experiment, $\text{Cu K}\alpha$ radiation (30 kV, 10 mA) was used and $\text{K}\beta$ radiation was attenuated with a Ni filter. The experiments were conducted without sample rotation at room temperature in the reflection mode at a rate of $10^\circ \text{ min}^{-1}$ for the anhydrous CD samples and at 5° min^{-1} for the hydrates. The diffractograms were also determined with an additive of standard silicon powder SRM 640d, and corresponding corrections were applied to the patterns obtained. The samples of anhydrous β CD were studied in a standard glass holder immediately after being taken out to air with a humidity of 20–40%.

To determine the cell parameters of polymorph III, the PXRD experiment was also held at an increased X-ray tube power (30 kV, 20 mA) with a scanning rate of $0.5^\circ \text{ min}^{-1}$ and a sample rotation of 80 rpm. To avoid the hydration of the β CD sample in the course of this experiment, the desiccants (freshly dried molecular sieves) were placed in the diffractometer camera. The indexing of patterns was performed using EXPO2014 software with further Rietveld refinement [29,30]. The cell parameters were found to have an M20 figure of merit value equal to 11.

2.4. Solution Calorimetry

The dissolution enthalpies and kinetics were measured at $298.15 \pm 0.01 \text{ K}$ using a semi-adiabatic calorimeter described earlier [31]. In this experiment, a sample of 30 mg was dissolved in 100 mL of distilled water. For each CD form, the dissolution experiment was carried out three times, and the average parameters of the calorimetric curves were calculated.

2.5. Infrared Spectroscopy

Infrared (IR) spectra were collected using the Vertex 70 (Bruker, Karlsruhe, Germany) Fourier-transform infrared spectrometer, which was purged with dry air before the experiment to remove the atmospheric humidity. The interferograms were recorded with 64 scans and a resolution of 2 cm^{-1} . The spectra of the solid samples were recorded using an attenuated total reflection MIRacle accessory with a germanium crystal (PIKE Tech., Madison WI, USA).

3. Results

3.1. Preparation of Polymorph III

The high-temperature polymorph (polymorph III) was prepared by heating the initial anhydrous β CD (polymorph I) to 508 K with further cooling to room temperature in an argon flow in the TG/DSC experiment. The corresponding TG/DSC curves are provided in

Figure 1. During the first heating of polymorph I, an endothermic effect was observed with an onset point at 495 K (Figure 1). The enthalpy of such effect was $\Delta H_{tr} = 16.5 \text{ kJ mol}^{-1}$. This effect was absent for the sample prepared by heating polymorph I to 508 K and cooling (Figure 1), and no peaks of phase transition could be seen in the corresponding DSC cooling curve in a separate TG/DSC experiment (Figures S7 and S8), which indicates the irreversibility of the observed transition.

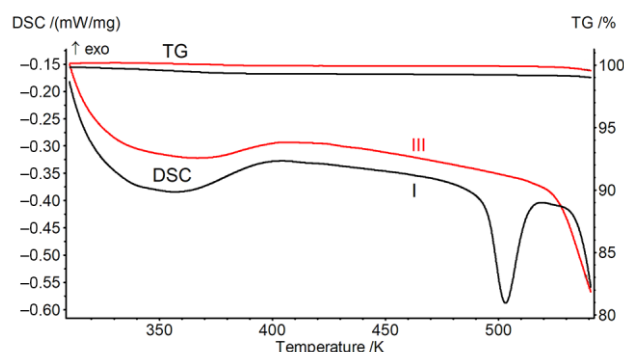


Figure 1. Curves of the TG/DSC analyses of polymorphs I and III with a heating rate of 10 K min^{-1} .

According to the TG data, β CD had no mass loss in the range of 473–513 K (Figure 1). Thus, the endothermic process at these temperatures corresponds to a polymorphic transition, leading to the formation of the new polymorph III. For this high-temperature polymorph III, the onset point of thermal destruction was 526 K, which is 8 K lower than that of the initial form. The lower thermal stability of polymorph III can be explained by its higher energy compared to that of the initial β CD form.

To differentiate between the endothermic polymorphic transition at 495 K and the thermal degradation of β CD, the dependence of the observed transition on the heating rate was determined in the DSC experiment, and the corresponding activation energy E_a was calculated using model-free and optimal model methods [32,33]. The experimental data and description of the calculation are provided in Supplementary Information (SI). For this transition, model-free Ozawa-Flynn-Wall and Friedman methods produced activation energies E_a equal to 430 and 350 kJ mol^{-1} , respectively, in the conversion range of 0.1–0.7. The optimal thermokinetic model is the Prout-Tompkins equation with $E_a = 430 \text{ kJ mol}^{-1}$ and a process order of $n = 1.92$. These E_a values are 3–4 times higher than the activation energy $E_a = 105 \text{ kJ mol}^{-1}$ of the β CD thermal degradation reaction [24], which confirms the different nature of the observed endothermic effect.

The changes in the crystal packing during the polymorphic transition were studied using the powder X-ray diffraction method. For this, the diffraction patterns were obtained for polymorph I, polymorph III, and the products resulting from saturation with water vapor at a relative humidity of 33% (water activity $a_w = 0.33$), recrystallization in water vapors at $a_w = 1.0$ (both at 298 K) and from an aqueous solution (Figure 2). For this experiment, polymorph III was prepared using two methods: heating polymorph I to 508 K and cooling in an argon flow and, on a larger scale, heating to 505 K and cooling in air. Both methods produce samples with nearly the same PXRD pattern (Figures 2b,c and S9).

The obtained diffractograms indicate the distinct packing of high-temperature polymorph III (Figure 2b,c) in comparison to that of the initial polymorph I (Figure 2a). The diffractogram of polymorph III was also compared (Figure S9) with the pattern simulated from the SCXRD data for a channel-type inclusion compound where disordered molecules of guest (chloramphenicol) and solvent (water) were removed using software methods [20]. This simulation and polymorph II exhibited coinciding intensive peaks at 2θ values of 7.2° and 11.9° , which in [17] are attributed to characteristic interplanar spacings of channel β CD packing. Polymorph III had no main PXRD peaks at these positions. Therefore, the crystal packing of polymorph III is not of the channel type.

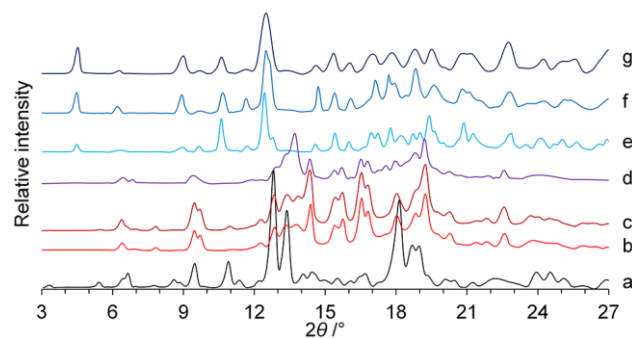


Figure 2. PXRD patterns at room temperature for (a) polymorph I; (b) polymorph III prepared by heating polymorph I to 508 K and cooling in an argon flow; (c) polymorph III prepared by heating polymorph I to 505 K and cooling in air; the products of polymorph III (d) hydration at water activity $a_w = 0.33$, (e) recrystallization in water vapors at $a_w = 1.0$, and (f) recrystallization from an aqueous solution at 298 K; (g) diffractogram of the saturated hydrate $\beta\text{CD}\cdot 11.2\text{H}_2\text{O}$.

The indexing of the high-temperature polymorph III diffractogram (Figure S5) for the sample prepared by heating polymorph I to 505 K and cooling it in air provided a triclinic cell with parameters of $a = 17.09 \text{ \AA}$, $b = 15.12 \text{ \AA}$, $c = 11.76 \text{ \AA}$, $\alpha = 109.5^\circ$, $\beta = 95.8^\circ$, $\gamma = 70.6^\circ$, and $R_{wp} = 5.466$ (Table 1). The cell volume of this high-temperature polymorph was $V = 2704 \text{ \AA}^3$, which is more compact than the initial dried βCD form, which had $V = 2894 \text{ \AA}^3$ [23]. For comparison, polymorph II had a hexagonal cell [17] with volume $V = 3069 \text{ \AA}^3$ (Table 2).

Table 2. Cell parameters of the anhydrous βCD polymorphs.

Polymorph	I	II	III ^a
Crystal system	Monoclinic	Hexagonal	Triclinic
Cell parameters	$a = 13.703 \text{ \AA}$ $b = 16.065 \text{ \AA}$ $c = 13.163 \text{ \AA}$ $\beta = 92.69^\circ$ [23]	$a = 15.34 \text{ \AA}$ $c = 15.06 \text{ \AA}$ [17]	$a = 17.09 \text{ \AA}$ $b = 15.12 \text{ \AA}$ $c = 11.76 \text{ \AA}$, $\alpha = 109.5^\circ$ $\beta = 95.8^\circ$ $\gamma = 70.6^\circ$
Cell volume, \AA^3	2894	3069	2704

^a Characteristic PXRD peaks were at 2θ values of 9.5, 13.4, 14.4, 15.7, 16.5, 19.2, and 22.6°.

At a water activity of $a_w = 0.33$ and 298 K, the hydration of polymorph II resulted in minor changes in its diffraction pattern (Figure 2d) without altering its main packing type. In saturated water vapors of $a_w = 1.0$, this polymorph forms a mixture of aqueous βCD solution and its solid hydrate, unlike the initial polymorph I, which remains in a solid state under these conditions [19,34]. The products of such recrystallization in water vapors (Figure 2e) and recrystallization of the same high-temperature polymorph III from an aqueous solution (Figure 2f) without drying have practically the same packing as the saturated hydrate $\beta\text{CD}\cdot 11.2\text{H}_2\text{O}$ prepared via the saturation of polymorph I at $a_w = 1.0$ (Figure 2g). Therefore, no chemical reactions occur in anhydrous βCD upon heating to 508 K, which is 5 K above the peak point of the polymorphic I→III transition. The absence of chemical changes was also confirmed by determination of IR spectra, which are the same for both polymorphs (Figure S6).

3.2. Dissolution Rate

Being the high-temperature form produced through the endothermic transition, polymorph III was expected to have a higher dissolution rate. To study the dissolution rate in water for this polymorph and the other studied anhydrous forms of βCD and dried HP βCD

for comparison, the method of solution calorimetry was chosen, which can estimate the time of fast dissolution processes [35].

The calorimetric curves were determined for the dissolution of polymorphs I and III, the amorphous forms of dried ball-milled β CD, and dried HP β CD (Figure 3). The corresponding dissolution time values t_{soln} and enthalpies ΔH_{soln} are provided in Table 3.

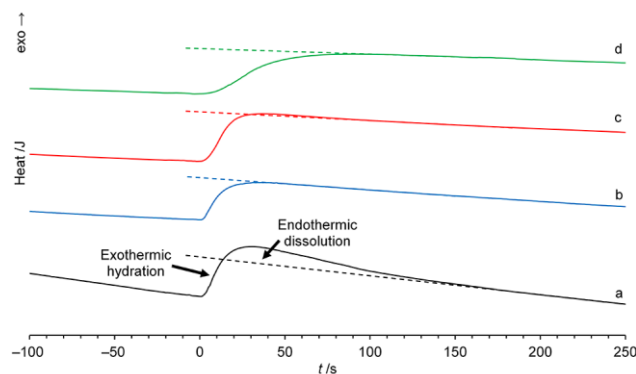


Figure 3. Calorimetric dissolution curves in water at 298 K for (a) polymorph I, (b) polymorph III, (c) anhydrous amorphous β CD, and (d) anhydrous HP β CD. The start of dissolution was at $t = 0$ s. The dotted lines are the extrapolations of the baselines after the end of the dissolution effects.

Table 3. Dissolution properties of the anhydrous forms of β CD and HP β CD in water at 298 K.

	Dissolution time t_{soln}/s	Solution enthalpy $\Delta H_{soln}/kJ mol^{-1}$
Polymorph I	190 ± 15	-86 ± 1
Polymorph III	43 ± 4	-94 ± 1
Amorphous β CD ^a	43 ± 4 (90 ± 10) ^b	-111 ± 1
HP β CD ^a	100 ± 10	-144 ± 1

^a PXRD patterns are provided in SI; ^b the total dissolution time with a prolonged endothermic effect having negligibly small enthalpy values.

The dissolution of polymorph I includes two processes: the exothermic hydration curve of anhydrous β CD and the endothermic dissolution of the β CD hydrate. These processes have been separately characterized elsewhere [36] and can be seen in the complex shape of the polymorph I dissolution curve (Figure 3a). This calorimetric curve demonstrates a rather fast exothermic effect in the first 35 s after the start of dissolution, with the next prolonged endothermic event lasting 155 s. The ratio of these thermal effects was 3.5:1 and corresponds to the values of the polymorph I solution enthalpy $\Delta H_{soln} = -86 \pm 1 kJ mol^{-1}$ and the literature's data [36] of $\Delta H_{soln} = -91 kJ mol^{-1}$ for the same anhydrous β CD form and $\Delta H_{soln} = +35 kJ mol^{-1}$ for saturated hydrate $\beta CD \cdot 12H_2O$, which results in a ratio of 3.6:1 for the β CD hydration and $\beta CD \cdot 12H_2O$ hydrate dissolution enthalpies. The composition of the saturated β CD hydrate is from the single crystal XRD [37]. This means that the hydration and hydrate dissolution events do not occur simultaneously to any significant extent but occur one after another.

The dissolution curve of polymorph III (Figure 3b) only displayed an exothermic effect with $\Delta H_{soln} = -94 \pm 1 kJ mol^{-1}$ within the first 43 s (Table 3). Therefore, its hydration and dissolution processes were simultaneous. The difference in the ΔH_{soln} values of polymorphs I and III at 298 K was $8 \pm 2 kJ mol^{-1}$ lower than the enthalpy of the polymorphic transition at $+16.5 kJ mol^{-1}$ with onset at 495 K, which may have been caused by the difference in the experimental temperatures (Figure 1). The amorphous β CD with a dissolution enthalpy of $\Delta H_{soln} = -111 \pm 1 kJ mol^{-1}$ showed the same dissolution time of 43 s as polymorph III, practically occurring in one exothermic step, followed by a very small but prolonged ($t_{soln} = 90 \pm 10$ s) endothermic effect, which only accounted for $\sim 3\%$ of the total dissolution enthalpy. This may have been caused by the formation of crystalline β CD hydrate from

a minor part of the initial amorphous sample, which had 17 kJ mol^{-1} higher energy than polymorph III.

The dissolution curve of anhydrous HP β CD with $\Delta H_{\text{soln}} = -144 \pm 1 \text{ kJ mol}^{-1}$ had the same shape as polymorph III but with a much higher dissolution time of $t_{\text{soln}} = 100 \text{ s}$ (Figure 3d, Table 2). Thus, the dissolution rate of polymorph III in water was close to that of amorphous β CD, being 4.4 and 2.3 times higher than that of the initial polymorph I and HP β CD, respectively, despite the latter being amorphous and its dissolution being more exothermic. A similar difference in the dissolution rates of these forms was also visually observed.

3.3. Thermodynamic Properties

Different properties for β CD polymorphs I and III were also observed in the DSC experiment where the dependences of their molar heat capacities $C_{p,m}$ on temperature T in the range of 343–463 K were determined. This range was chosen because it excludes the influence of water traces in dried argon used to purge the CD samples. The obtained plots of $C_{p,m}$ vs. T are provided in Figure 4, and the values of $C_{p,m}$ at each studied temperature are provided in SI. The molar heat capacity of the initial polymorph I can be described using the equation $C_{p,m} = -1219 + 10.36T - 0.00623T^2$. This equation extrapolated to the temperature $T = 298 \text{ K}$ results in $C_{p,m} = 1316 \pm 13 \text{ J K}^{-1} \text{ mol}^{-1}$, which is slightly lower than $1342 \pm 10 \text{ J K}^{-1} \text{ mol}^{-1}$ measured earlier at the same temperature [38]. The molar heat capacity of polymorph III can be described as $C_{p,m} = -884 + 9.05T - 0.00478T^2$. Hence, the molar heat capacity of polymorph III is higher than that of polymorph I in the studied temperature range (Figure 4).

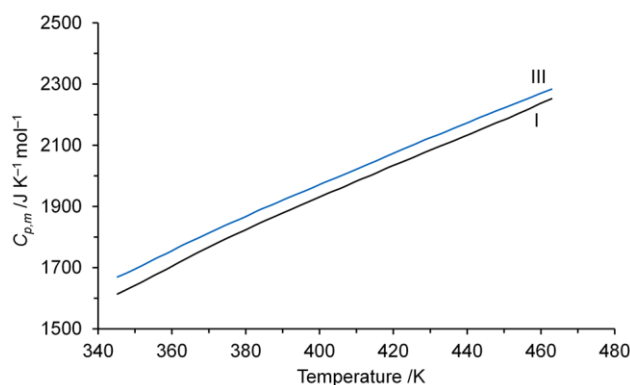


Figure 4. Dependence of molar heat capacity on temperature for β CD polymorphs I and III.

The enthalpy of the I \rightarrow III transition ΔH_{tr} at 298 K can be estimated using Kirchoff's law with a value of $\Delta H_{\text{tr}}(495 \text{ K}) = 16.5 \text{ kJ mol}^{-1}$ determined in the DSC experiment (Figure 1) and the difference in the heat capacities $\Delta C_{p,m}$ of polymorphs I and III:

$$\Delta H_{\text{tr}}(298 \text{ K}) = \Delta H_{\text{tr}}(495 \text{ K}) + \int_{495}^{298} \Delta C_{p,m}(T) dT = 7.1 \left(\frac{\text{kJ}}{\text{mol}} \right)$$

The calculated value of $\Delta H_{\text{tr}}(298 \text{ K})$ coincides with the difference in the dissolution enthalpies of polymorphs I and III in water at 298 K, which is equal to $8 \pm 2 \text{ kJ mol}^{-1}$ (Table 2).

Since the endothermic process in anhydrous β CD at 495 K is the transition from polymorph I to polymorph III, followed by the melting of β CD at 774 K [24], the polymorphic transition is enantiotropic with a Gibbs energy transition value of zero $\Delta G_{\text{tr}}(495 \text{ K}) = 0$, according to the Burger and Ramberger heat-of-transition rule [39]. Hence, the value of the polymorphic

transition entropy at its onset point is equal to $\Delta S_{\text{tr}}(495 \text{ K}) = 33 \text{ J mol}^{-1} \text{ K}^{-1}$. Thus, the entropy of the I→III transition at 298 K can be calculated as follows:

$$\Delta S_{\text{tr}}(298 \text{ K}) = \Delta S_{\text{tr}}(495 \text{ K}) + \int_{495}^{298} \frac{\Delta C_{p,m}(T)}{T} dT = 8.2 \left(\frac{\text{J}}{\text{mol}\cdot\text{K}} \right)$$

This produces a positive value of transition Gibbs energy at the standard temperature, $\Delta G_{\text{tr}}(298 \text{ K}) = 4.7 \text{ kJ mol}^{-1}$, which means that polymorph III has a higher Gibbs energy than polymorph I at 298 K. Such relationship can explain the higher dissolution rate of polymorph III and, therefore, its higher bioavailability.

3.4. Affinity for Water

To compare the water affinity of polymorph III with that of polymorph I and HP β CD, we measured the hydration isotherms for polymorph III and HP β CD using their equilibration with water vapors of fixed humidity at 298 K, followed by the gravimetric determination of the hydrates' composition. The hydration isotherm of polymorph I has been determined elsewhere [34]. The isotherms were fitted using the Hill equation as described earlier [40]. The equation used, and the approximation parameters are provided in SI. These are the inclusion capacity S , water activity at 50% saturation $a_{0.55}$ (which is a hydration threshold), and cooperativity parameter for separate inclusion steps.

The hydration of polymorph III occurs in two steps (Figure 5b), corresponding to the inclusion capacity S of 2.5 and 1.6 mol of water per mol of β CD, with hydration thresholds $a_{0.55}$ at 0.09 and 0.30, respectively. Such steps mean that the hydration of polymorph III produces a phase transition, which may be induced by the inclusion inside the β CD cavity because the uptake of four water molecules at $a_w = 0.33$ does not produce significant changes in the polymorph III PXRD pattern (Figure 2d). For comparison, 4.5 and 7 water molecules have such inclusion types in β CD·9.4H₂O and β CD·12.3H₂O single crystals, respectively [21]. The hydration of polymorph III at $a_w = 0.43$ produces a mixture of aqueous solution and crystalline β CD hydrate with a total β CD/water molar ratio of 1:20.5, where the liquid phase is visually observed. Such behavior was not observed under the same conditions for polymorph I, which could not absorb more water than needed to form its hydrates in two steps (Figure 5b), corresponding to the inclusion capacity S of 9.2 and 2.2 mol per mol of β CD with a hydration threshold $a_{0.55}$ at 0.26 and 0.97, respectively [34].

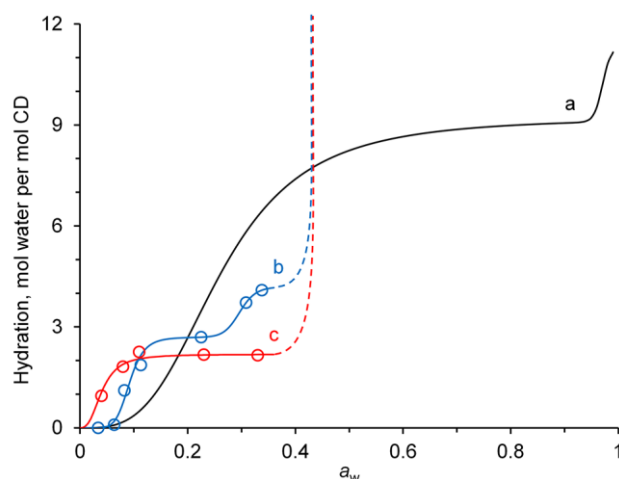


Figure 5. Water sorption isotherms on (a) polymorph I [34] and (b) polymorph III, and on (c) anhydrous HP β CD at 298 K. $T = 298 \text{ K}$. The dotted line corresponds to the formation of a liquid solution.

The isotherm of HP β CD hydration (Figure 5c) performed only one step with a lower hydration capacity of $S = 2.2 \text{ mol mol}^{-1}$ and hydration threshold of $a_{0.55} = 0.04$. This isotherm also became vertical at $a_w = 0.43$ with HP β CD providing a liquid drop of its aqueous solution. Thus, this β CD derivative is more water soluble than the previously

studied HP β CD, with a lower substitution ratio of 0.6, which does not dissolve in water vapors even at $a_w = 1$ [41].

The affinities of the studied CDs for water can be characterized by their hydration Gibbs energy ΔG_h , which were calculated for each hydration step using the equation:

$$\Delta G_h = RT \ln a_{0.5S} \quad (1)$$

This equation provides the Gibbs energy [40] of water transfer from its pure liquid to stable hydrate form with the inclusion capacity S . The values of ΔG_h for the first and second hydration step for polymorph III were -5.9 and -3.0 kJ per 1 mol of water, respectively. HP β CD had a value of $\Delta G_h = -7.9$ kJ mol $^{-1}$. For comparison, two steps of polymorph I hydration correspond to ΔG_h values of -3.3 and -0.1 kJ mol $^{-1}$, respectively [34]. Therefore, the affinity for water changes in the following order: HP β CD > polymorph III > polymorph I. While HP β CD is highly soluble in water (>600 mg mL $^{-1}$) [42], a similarly high solubility could be expected for polymorph III. Still, the equilibrium solubility of polymorph III is restricted by the ability of β CD to recrystallize into its saturated hydrate form, resulting in a low solubility of 18.4 mg mL $^{-1}$ [42], which was visually observed for polymorph III in water vapors at an activity of $a_w = 0.43$ as mentioned above. Such dissolution-crystallization behavior can be useful for the preparation of inclusion compounds in pastes using a small amount of water or for the quick removal of undesirable compounds from an aqueous solution via their complexation with β CD using much faster dissolution of polymorph III. This property renders polymorph III a promising alternative to the more expensive synthetic derivatives of cyclodextrins.

4. Conclusions

The new polymorph III of β -cyclodextrin was prepared through an endothermic transition by heating the dried commercial form of β -cyclodextrin (polymorph I). The absence of chemical changes in β -cyclodextrin using this treatment was proven by its IR spectra and PXRD patterns after its hydration. Polymorph III has a triclinic cell with an essentially different packing than that of polymorph I. Polymorph III is energy-rich: the I \rightarrow III polymorphic transition has a positive enthalpy of $+8$ kJ mol $^{-1}$ and a Gibbs energy of $+4.7$ kJ mol $^{-1}$ at 298 K. The dissolution of polymorph III in liquid water is 4.3 and 2.3 times faster than the dissolution of polymorph I and hydroxypropyl- β -cyclodextrin (HP β CD), respectively, under the same conditions. Polymorph III dissolves in water vapors at the same humidity as the highly water-soluble HP β CD and has a higher affinity for water with a more negative hydration Gibbs energy than polymorph I. Thus, the new polymorph can be used for the preparation of inclusion compounds in pastes or for the quick removal of undesirable compounds from water, being a cheaper alternative to the chemically modified β -cyclodextrin.

Supplementary Materials: The following supporting information can be downloaded at: <https://www.mdpi.com/article/10.3390/chemistry6010003/s1>, Figure S1–S3: Thermokinetic analysis of the polymorphic transition; Figure S4: PXRD analysis of amorphous β CD and HP β CD Table S1 and Figure S5: PXRD data and indexing graph for β CD polymorph III; Figure S6: FTIR spectra for β CD polymorphs I and III; Figures S7–S8: Curves of the full-cycle TG/DSC analysis of β CD; Figure S9: PXRD patterns of β CD polymorph III prepared by different methods and comparison with simulation from SCXRD data (WEWTOJ); Table S2: Molar heat capacity dependence on temperature for polymorphs I and III; Hill equation used for approximation of each isotherm step; Table S3: Parameters of hydration isotherms for β CD polymorphs and HP β CD. Supplementary Information: The following supporting information (thermokinetic analysis of the polymorphic transition; PXRD data for polymorph III and amorphous β CD/HP β CD; IR spectra for β CD polymorphs I and III; Molar heat capacity data for β CD polymorphs I and III.

Author Contributions: A.K.G. conceptualization, formal analysis, writing—original draft; I.S.B. investigation; S.M.T. investigation; M.A.Z. writing—review and editing; V.V.G. supervision, writing—review and editing. All authors have read and agreed to the published version of the manuscript.

Funding: The work was supported by the RSF grant no. 22-23-00367.

Data Availability Statement: The data that support the findings of this study are available from the corresponding author upon reasonable request.

Conflicts of Interest: The authors declare no conflicts of interest.

References

1. Fenyvesi, E.; Sente, L. Cyclodextrin in Starchy Foods. *Acta Aliment.* **2021**, *50*, 417–432. [[CrossRef](#)]
2. Morin-Crini, N.; Fourmentin, S.; Fenyvesi, É.; Lichtfouse, E.; Torri, G.; Fourmentin, M.; Crini, G. 130 Years of Cyclodextrin Discovery for Health, Food, Agriculture, and the Industry: A Review. *Environ. Chem. Lett.* **2021**, *19*, 2581–2617. [[CrossRef](#)]
3. Gonzalez-Gaitano, G.; Isasi, J.R.; Velaz, I.; Zornoza, A. Drug Carrier Systems Based on Cyclodextrin Supramolecular Assemblies and Polymers: Present and Perspectives. *Curr. Pharm. Des.* **2017**, *23*, 411–432. [[CrossRef](#)] [[PubMed](#)]
4. Ferreira, L.; Mascarenhas-Melo, F.; Rabaça, S.; Mathur, A.; Sharma, A.; Giram, P.S.; Pawar, K.D.; Rahdar, A.; Raza, F.; Veiga, F.; et al. Cyclodextrin-Based Dermatological Formulations: Dermopharmaceutical and Cosmetic Applications. *Colloids Surf. B Biointerfaces* **2023**, *221*, 113012. [[CrossRef](#)] [[PubMed](#)]
5. Puskás, I.; Sente, L.; Szócs, L.; Fenyvesi, É. Recent List of Cyclodextrin-Containing Drug Products. *Period. Polytech. Chem. Eng.* **2023**, *67*, 11–17. [[CrossRef](#)]
6. Kravtsova, A.A.; Skuredina, A.A.; Malyshev, A.S.; Le-Deygen, I.M.; Kudryashova, E.V.; Budynina, E.M. The Solubility Studies and the Complexation Mechanism Investigations of Biologically Active Spiro[Cyclopropane-1,3'-Oxindoles] with β -Cyclodextrins. *Pharmaceutics* **2023**, *15*, 228. [[CrossRef](#)]
7. Zornoza, A.; Vélaz, I.; González-Gaitano, G.; Martínez-Ohárriz, M.C. A Comprehensive Study of Gemfibrozil Complexation with β -Cyclodextrins in Aqueous Solution Using Different Analytical Techniques. *Int. J. Mol. Sci.* **2022**, *23*, 16119. [[CrossRef](#)]
8. Soe, H.M.S.H.; Chamni, S.; Mahalabutr, P.; Kongtaworn, N.; Rungrotmongkol, T.; Jansook, P. The Investigation of Binary and Ternary Sulfobutylether- β -Cyclodextrin Inclusion Complexes with Asiaticoside in Solution and in Solid State. *Carbohydr. Res.* **2020**, *498*, 108190. [[CrossRef](#)]
9. Censi, R.; Di Martino, P. Polymorph Impact on the Bioavailability and Stability of Poorly Soluble Drugs. *Molecules* **2015**, *20*, 18759–18776. [[CrossRef](#)]
10. Li, L.; Yin, X.-H.; Diao, K.-S. Improving the Solubility and Bioavailability of Pemafibrate via a New Polymorph Form II. *ACS Omega* **2020**, *5*, 26245–26252. [[CrossRef](#)]
11. Loftsson, T.; Fulop, Z. Preparation of Solid Cyclodextrin Complexes for Ophthalmic Active Pharmaceutical Ingredient Delivery. U.S. Patent 1,113,531,1B2, 5 October 2021.
12. Mentzafos, D.; Bethanis, K. β -Cyclodextrin Dimeric Inclusion Complexes: A Review of Some Crystal Structure Aspects. In *Cyclodextrins: Synthesis, Chemical Applications and Role in Drug Delivery*; Ramirez, F.G., Ed.; Nova Science: New York, NY, USA, 2015; Chapter 8.
13. Ceborska, M. Structural Investigation of Solid State Host/Guest Complexes of Native Cyclodextrins with Monoterpenes and Their Simple Derivatives. *J. Mol. Struct.* **2018**, *1165*, 62–70. [[CrossRef](#)]
14. Harata, K. Crystallographic Study of Cyclodextrins and Their Inclusion Complexes. In *Cyclodextrins and Their Complexes: Chemistry, Analytical Methods, Applications*; Dodziuk, H., Ed.; Wiley-VCH: Weinheim, Germany, 2006; pp. 147–198.
15. Shih, T.-W.; Hsu, C.-L.; Chen, L.-Y.; Huang, Y.-C.; Chen, C.-J.; Inoue, Y.; Sugiyama, T. Optical Trapping-Induced New Polymorphism of β -Cyclodextrin in Unsaturated Solution. *Cryst. Growth Des.* **2021**, *21*, 6913–6923. [[CrossRef](#)]
16. Panova, I.G.; Zhukova, E.K.; Matukhina, E.V.; Topchieva, I.N. Receptor Properties of Nanoporous Structures Based on β -Cyclodextrin. *Nanotechnologies Russ.* **2010**, *5*, 304–312. [[CrossRef](#)]
17. Panova, I.G.; Matukhina, E.V.; Gerasimov, V.I.; Topchieva, I.N. Non-Covalent Columnar Cyclodextrin-Based Structures. *Colloid J.* **2006**, *68*, 66–78. [[CrossRef](#)]
18. Martini, A.; Torricelli, C.; Muggetti, L.; De Ponti, R. Use of Dehydrated Beta-Cyclodextrin as Pharmaceutical Excipient. *Drug Dev. Ind. Pharm.* **1994**, *20*, 2381–2393. [[CrossRef](#)]
19. Gorbachuk, V.V.; Gatiatulin, A.K.; Ziganshin, M.A.; Gubaidullin, A.T.; Yakimova, L.S. Unusually High Efficiency of β -Cyclodextrin Clathrate Preparation by Water-Free Solid-Phase Guest Exchange. *J. Phys. Chem. B* **2013**, *117*, 14544–14556. [[CrossRef](#)] [[PubMed](#)]
20. Ramos, A.I.; Braga, T.M.; Silva, P.; Fernandes, J.A.; Ribeiro-Claro, P.; Lopes, M.d.F.S.; Paz, F.A.A.; Braga, S.S. Chloramphenicol-cyclodextrin Inclusion Compounds: Co-Dissolution and Mechanochemical Preparations and Antibacterial Action. *CrystEngComm* **2013**, *15*, 2822. [[CrossRef](#)]
21. Steiner, T.; Koellner, G. Crystalline β -Cyclodextrin Hydrate at Various Humidities: Fast, Continuous, and Reversible Dehydration Studied by X-Ray Diffraction. *J. Am. Chem. Soc.* **1994**, *116*, 5122–5128. [[CrossRef](#)]
22. Sala, A.; Hoossen, Z.; Bacchi, A.; Caira, M.R. Two Crystal Forms of a Hydrated 2:1 β -Cyclodextrin Fluconazole Complex: Single Crystal X-Ray Structures, Dehydration Profiles, and Conditions for Their Individual Isolation. *Molecules* **2021**, *26*, 4427. [[CrossRef](#)]
23. Osel'skaya, V.Y.; Gatiatulin, A.K.; Klimovitskii, A.E.; Ziganshin, M.A.; Gorbachuk, V.V. Competing Role of Water in Inclusion of Indomethacin and Volatile Organic Compounds by Native Cyclodextrins. *Macroheterocycles* **2022**, *15*, 174–185. [[CrossRef](#)]

24. Gatiatulin, A.K.; Grishin, I.A.; Buzyurov, A.V.; Mukhametzyanov, T.A.; Ziganshin, M.A.; Gorbachuk, V.V. Determination of Melting Parameters of Cyclodextrins Using Fast Scanning Calorimetry. *Int. J. Mol. Sci.* **2022**, *23*, 13120. [[CrossRef](#)] [[PubMed](#)]
25. Giordano, F.; Novak, C.; Moyano, J.R. Thermal Analysis of Cyclodextrins and Their Inclusion Compounds. *Thermochim. Acta* **2001**, *380*, 123–151. [[CrossRef](#)]
26. Jansook, P.; Ogawa, N.; Loftsson, T. Cyclodextrins: Structure, Physicochemical Properties and Pharmaceutical Applications. *Int. J. Pharm.* **2018**, *535*, 272–284. [[CrossRef](#)] [[PubMed](#)]
27. Lan Pham, T.; Usacheva, T.R.; Alister, D.A.; Thu Ha Nguyen, T.; Tukumova, N.V.; Kuranova, N.N.; Minh Vu, X.; My Hanh Le, T.; Tung Nguyen, Q.; Lam Tran, D. Thermodynamic Parameters and Quantum Chemical Calculations of Complex Formation between Rutin and 2-Hydroxypropyl- β -Cyclodextrin in Water-Ethanol Solvents. *J. Mol. Liq.* **2022**, *366*, 120324. [[CrossRef](#)]
28. Nagrimanov, R.N.; Samatov, A.A.; Buzyurov, A.V.; Kurshev, A.G.; Ziganshin, M.A.; Zaitsau, D.H.; Solomonov, B.N. Thermochemical Properties of Mono- and Di-Cyano-Aromatic Compounds at 298.15 K. *Thermochim. Acta* **2018**, *668*, 152–158. [[CrossRef](#)]
29. Altomare, A.; Cuocci, C.; Giacobuzzo, C.; Moliterni, A.; Rizzi, R.; Corriero, N.; Falcicchio, A. EXPO2013: A Kit of Tools for Phasing Crystal Structures from Powder Data. *J. Appl. Crystallogr.* **2013**, *46*, 1231–1235. [[CrossRef](#)]
30. McCusker, L.B.; Von Dreele, R.B.; Cox, D.E.; Louër, D.; Scardi, P. Rietveld Refinement Guidelines. *J. Appl. Crystallogr.* **1999**, *32*, 36–50. [[CrossRef](#)]
31. Varfolomeev, M.A.; Abaidullina, D.I.; Solomonov, B.N.; Verevkin, S.P.; Emel'yanenko, V.N. Pairwise Substitution Effects, Inter- and Intramolecular Hydrogen Bonds in Methoxyphenols and Dimethoxybenzenes. Thermochemistry, Calorimetry, and First-Principles Calculations. *J. Phys. Chem. B* **2010**, *114*, 16503–16516. [[CrossRef](#)]
32. Vyazovkin, S. *Isoconversional Kinetics of Thermally Stimulated Processes*; Springer: Berlin/Heidelberg, Germany, 2015; p. 239.
33. Vyazovkin, S.; Burnham, A.K.; Criado, J.M.; Pérez-Maqueda, L.A.; Popescu, C.; Sbirrazzuoli, N. ICTAC Kinetics Committee Recommendations for Performing Kinetic Computations on Thermal Analysis Data. *Thermochim. Acta* **2011**, *520*, 1–19. [[CrossRef](#)]
34. Gatiatulin, A.K.; Ziganshin, M.A.; Yumaeva, G.F.; Gubaidullin, A.T.; Suwińska, K.; Gorbachuk, V.V. Using Water-Mimic Organic Compounds to Activate Guest Inclusion by Initially Dry Beta-Cyclodextrin. *RSC Adv.* **2016**, *6*, 61984–61995. [[CrossRef](#)]
35. Kayaert, P.; Li, B.; Jimidar, I.; Rombaut, P.; Ahssini, F.; Van den Mooter, G. Solution Calorimetry as an Alternative Approach for Dissolution Testing of Nanosuspensions. *Eur. J. Pharm. Biopharm.* **2010**, *76*, 507–513. [[CrossRef](#)] [[PubMed](#)]
36. Bilal, M.; de Brauer, C.; Claudy, P.; Germain, P.; Letoffe, J. β -Cyclodextrin hydration: A calorimetric and gravimetric study. *Thermochim. Acta* **1995**, *249*, 63–73. [[CrossRef](#)]
37. Lindner, K.; Saenger, W. Crystal and Molecular Structure of Cyclohepta-Amylose Dodecahydrate. *Carbohydr. Res.* **1982**, *99*, 103–115. [[CrossRef](#)]
38. Briggner, L.-E.; Wadsö, I. Heat Capacities of Maltose, Maltotriose, Maltotetrose and α -, β -, and γ -Cyclodextrin in the Solid State and in Dilute Aqueous Solution. *J. Chem. Thermodyn.* **1990**, *22*, 1067–1074. [[CrossRef](#)]
39. Burger, A.; Ramberger, R. On the Polymorphism of Pharmaceuticals and Other Molecular Crystals. I. *Mikrochim. Acta* **1979**, *72*, 259–271. [[CrossRef](#)]
40. Gorbachuk, V.V.; Tsifarkin, A.G.; Antipin, I.S.; Solomonov, B.N.; Konovalov, A.I. Influence of the Guest Molecular Size on the Thermodynamic Parameters of Host–Guest Complexes between Solid Tert-Butylcalix[4]Arene and Vapours of Organic Compounds. *Mendeleev Commun.* **1999**, *9*, 11–13. [[CrossRef](#)]
41. Ogata, F.; Hayabuchi, R.; Saenjum, C.; Nakamura, T.; Kawasaki, N. Adsorption Behavior of Water on Virgin and Modified Cyclodextrin. *Yakugaku Zasshi* **2020**, *140*, 1165–1173. [[CrossRef](#)]
42. Loftsson, T.; Sigurdsson, H.H.; Jansook, P. Anomalous Properties of Cyclodextrins and Their Complexes in Aqueous Solutions. *Materials* **2023**, *16*, 2223. [[CrossRef](#)]

Disclaimer/Publisher's Note: The statements, opinions and data contained in all publications are solely those of the individual author(s) and contributor(s) and not of MDPI and/or the editor(s). MDPI and/or the editor(s) disclaim responsibility for any injury to people or property resulting from any ideas, methods, instructions or products referred to in the content.